Near Surface Geophysics, 2008, xxx-xxx

Two-dimensional inverse filtering for the rectification of the magnetic gradiometry signal

G.A. Tassis [1*], R.O. Hansen[2], G.N. Tsokas[1], C.B. Papazachos[1] and P.I. Tsourlos[1]

[1] *Applied Geophysical Laboratory, Aristotle University of Thessaloniki, 54124 Thessaloniki, Greece*
[2] *EDCON-PRJ, Inc., 171 South Van Gordon St, Suite E, Lakewood, Colorado 80228, USA*

Received January 2006, revision accepted November 2007

ABSTRACT

The magnetic difference, the quantity measured by magnetic gradiometers, is considered to be the convolution between a function that controls the anomaly pattern and another that controls the strength signal. These are called shape and amplitude functions, respectively. They are distinct and analytically determined; thus, after the assessment of a suitable model, its shape function can be inverted to serve as a filter. If this filter is next convolved with the measured field, a series of amplitude functions is recovered, provided that the subsurface structures can be simulated by a combination of a number of models similar to the one whose anomaly was inverted. The recovered series is essentially the subsurface distribution of the amplitude function.

Alternatively, the scheme can be viewed as a transformation of the original field of magnetic differences. The signals, transformed in this context, comprise rectified monopolar versions of the originals, positioned directly above the centre of the targets. Furthermore, their amplitude is a measure of the magnetization of the targets. Thus, the new anomalies can be viewed as a kind of magnetization or susceptibility mapping. Inversion filters are computed in the Wiener mode by inverting the shape function of the anomalies caused by vertical sided finite prisms. This particular model is appropriate for a wide variety of targets that are commonly met in archaeological prospecting.
Converting the magnetic signal from the dual lobe pattern to single monopolar anomalies cause them to resemble the usual outcome of resistivity exploration. In this context, this work aims to form a scheme that makes the magnetic gradiometry outcome directly comparable to the outcome of resistivity mapping. Furthermore, it can be applied without contradicting or excluding any other processing operation.

The method is implemented in a FORTRAN program that is reasonably user- friendly. The efficiency of the scheme is tested both on synthetic and real data sets.

INTRODUCTION

Magnetic prospecting, either in the form of total field measurements or gradiometry, proved long ago to be a suitable method for investigating buried antiquities. Also, resistivity mapping proved to be successful for archaeological prospection. The mapped resistivities are usually depicted in image form, where the recorded anomalies are centred directly above the buried structures that caused them, provided that certain types of electrode arrays are employed (Aspinall and Lynam 1973). Also, for specific electrode arrays, the areal extent of the signal is representative of the horizontal dimensions of the buried body. Both these properties produce the images obtained by resistivity mapping that resemble the plan view of the concealed antiquities. The result of magnetic prospecting is also customarily presented in image form with great success (Scollar *et al.* 1986).

In magnetic prospecting, a number of techniques can be applied in an automatic mode to yield the spatial distribution of parameters that describe the source. Searching for targets not in the archaeological context and in particular in aeromagnetic data, a number of automatic techniques are used; for example, Werner deconvolution (Hartman *et al.* 1971), 3D Euler deconvolution (Reid *et al.* 1990), multiple source Werner deconvolution (Hansen and Simmonds 1993) and the 3D analytic signal technique (Roest *et al.* 1992). However, these schemes are not popular in archaeological geophysics because of the special aspects of the archaeological problem. Nonetheless, they may be used in order to solve specific problems, such as determining the burial depth (Tsokas and Hansen 1995; Tsokas and Hansen 2000). The wavelet transform-based multiscale analysis also helps to discard

* tassisl@geo.auth.gr

undesired components of the signal (Daubechies 1990; Fedi and Quarta 1998; Mallat 1999; Fleming *et al.* 2000).

The disturbances of the Earth's magnetic field caused by buried structures create signals that have both positive and negative lobes and are generally asymmetric. In other words, the magnetic signal does not give directly an indication of the exact location of the centre of the disturbing source or of its horizontal dimensions. Several mathematical methodologies have therefore been proposed to reduce the asymmetry of the magnetic signal. Usually, the signal is transformed into a monopolar form by reduction to the north magnetic pole (Baranov and Naudy 1964; Blakely 1995) or to pseudo gravimetric anomalies (Baranov 1957). The so-called 'terracing' technique (Cordell and McCafferty 1989) is also aimed at the same goal. The product is a kind of equivalent source derived from measured magnetic data (Blakely 1995). Also, inverse filtering proposed by Tsokas *et al.* (1991) and Tsokas and Papazachos (199 2) reduces the magnetic signal into a monopolar form whose amplitude is directly related to the magnetization of the causative body, i.e., to the susceptibility contrast of the source, provided that the magnetization is along a stable direction.

All three of the aforementioned schemes aim at a three-fold target: the resulting magnetic maps should provide an outline of the horizontal dimensions of the disturbing bodies, present their centres at their actual locations and give an estimate of the susceptibility contrast. Of course, the reliability of the products is a prerequisite.

The present work deals with the rectification of the gradiometer anomalies based on the construction of the suitable inverse filters. It can be considered as an extension of the work done so far for magnetic total field data, whose full theoretical and technical documentation can be found in the work of Tsokas and Papazachos (1992).

The application of inverse filters in the geophysical search for antiquities has been proposed by Karousova and Karous (1989). They have used the equations of Logacev and Zacharov (1973) to compute inverse filters based on vertical cylinders and infinite prisms. Tsokas *et al.* (1991) developed this procedure a step further by computing filters based on finite prisms and applying them to all of the profiles composing the grid of the geophysical search. This results into a pseudo two-dimensional procedure. They also commented on the filter's truncation length. Tsokas and Papazachos (1992) have studied the full 2D procedure and have constructed the relevant FORTRAN program (Papazachos and Tsokas 1993). They also tested the efficiency of the method on synthetic and real data. An investigation of the inferred resolution, the influence of the burial depth and the use of an improper filter with respect to the target was presented by Tsokas (1993). The main conclusion was that a global filter can be used, since almost all of the structures that archaeological prospection seeks can be simulated by ensembles of vertical sided prisms. Furthermore, even if the structures are more like cylinders and spheres, not much is lost since the anomaly pattern is mainly governed by the inclination of the normal field and the azimuth of the measuring profile.

Thus, the present work is largely dependent on the referred papers but also considers the gradiometry case. The outcome is the formulation of the mathematical algorithm and the construction of the relevant software. The convolutional model has been appropriately modified to fit the new concept. It is expected to offer images of better quality due to the advantages that the differential data inherently possess: that fewer errors are introduced since the diurnal variation correction is not required and more importantly, that the effects of regional fields are strongly suppressed.

The main aim is to convert the magnetic gradiometry data into a form that is more easily interpretable and understood by non experts, in other words, to have a precise image that resembles the plan view of the concealed antiquities (Scollar *et al.* 1986). This approximates the plan view if excavation had taken place and the plan views of the unearthed ruins were drawn.

THE CONVOLUTIONAL MODEL

The presentation of the basic theory of this paragraph follows the concept given by Tsokas and Papazachos (1992). Thus, parts of this documentation have been quoted from that work.

Tsokas and Papazachos (1990, 1992) used a previously defined formula (Grant and West 1965; McGrath and Hood 1973) in order to define the magnetic anomaly, ΔT, of any block-like body, as the accumulation of the contribution of thin plates. That is,

$$\Delta T(x,y) = J \cdot s \cdot b \cdot c \cdot \left[f(x, y+Y) - f(x, y-Y) \right], \tag{1}$$

Where J and s are the intensity of magnetization and the thickness of the block, respectively. The terms b and c are trigonometric functions of the angles defining the directions of the normal and produced field. The function f relates the geometric features of the block with the distances to the point of observation, i.e., it is a Green's function.

Equation (1) can be written as the product of two functions, say D and R. If we define

$$D = J, \tag{2}$$

we can reasonably term this factor as the 'amplitude' function because it modulates the strength of the anomaly. The remainder, comprise the function

$$R(x,y) = s \cdot b \cdot c \cdot \sum_{j=1}^{n} \left[f(x, y+Y) - f(x, y-Y) \right], \tag{3}$$

which can be termed as the 'shape' function since it controls the shape of the anomaly. Thus, considering that the bodies' centre is at the origin of the coordinate system (0, 0), the anomaly at a data point (x, y) can be expressed as

$$\Delta T(x,y) = D \cdot R(x,y). \tag{4}$$

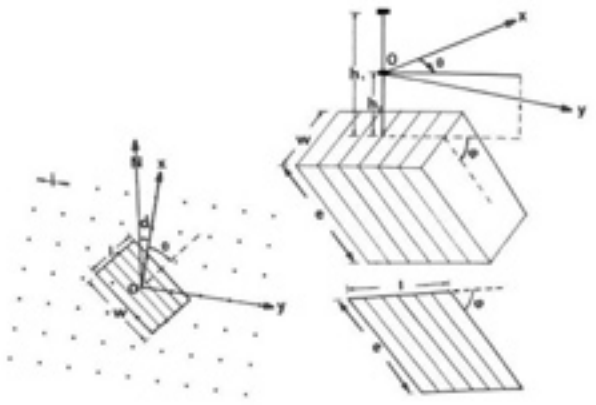

Figure 1
Coordinate system and prism configuration used throughout this work. The coordinate system of the data is oxy, **d** is the declination of magnetic north from the x-axis and θ is the prism's dip direction with respect to the x-axis. The burial depths are denoted by $\mathbf{h}_1$ and $\mathbf{h}_2$, **e** is the depth extent measured along the dip of the prism and **w** and **l** are the dimensions of its upper rectangular side. If the dip angle, φ, is selected to be equal to 90°, then we have a vertical sided prism. The term I represents the sampling interval. (Tsokas and Papazachos 1992; modified by Tassis 2005).

In order to proceed to the convolutional model we make the assumption that the magnetization is of an induced type or at least, is of known direction. Then, an ensemble of bodies placed at the same depth at points

$$x_i = I\Delta x\,; \quad i = L_1,\ldots,L_2$$
$$y_m = m\Delta y\,; \quad m = M_1,\ldots,M_2$$

can be considered. Figure 1 shows the geometrical scaffold of the proposed notation.

Assuming the validity of the superposition principle, the total field anomaly at each point (x_i, y_i) is

$$\Delta T(x_i, y_j) = \sum_{l=L_1}^{L_2} \sum_{m=M_1}^{M_2} D_{l,m} \cdot R(x_i - x_l, y_j - y_m) \qquad (5)$$
$$i = L_1,\ldots,L_2 \quad m = M_1,\ldots,M_2$$

Using matrix notation,

$$T_{ij} = \Delta T(x_i, y_j),\ D_{lm} = D(x_l, y_m)$$

and

$$R_{i-l,j-m} = R(x_i - x_l, y_j - y_m)$$

the total field anomaly is written as

$$T_{ij} = \sum_{l=L_1}^{L_2} \sum_{m=M_1}^{M_2} D_{lm} \cdot R_{i-l,j-m} \qquad (6)$$

or more simply

$$\mathbf{T} = \mathbf{D} * \mathbf{R} \qquad (7)$$

where the symbol * denotes convolution.
The 'amplitude' function (magnetization) is

$$\mathbf{D} = \mathbf{T} * \mathbf{R}^{-1} \qquad (8)$$

given that $\mathbf{R} * \mathbf{R}^{-1} = \mathbf{I}$ (**I** is the unit element of convolution). Usually, $\mathbf{R}^{-1}$ has an infinite length. In practice, however, we want to determine a truncated version of the inverse filter, $\overline{\mathbf{R}}^{-1}$, because there is no practical use for an infinite series. Such a filter can be provided by the minimization of

$$\mathbf{E}^2 = (\mathbf{R} * \overline{\mathbf{R}}^{-1} - \mathbf{I})^2$$

and is given (Kanasewich 1981) by

$$\sum_{l=L_1}^{L_2} \sum_{m=M_1}^{M_2} R^{-1}_{i,j} \cdot A_{k-i,l-j} = R_{-k,-l} \qquad (9)$$
$$k = M_1,\ldots,M_2 \quad l = L_1,\ldots,L_2$$

where **A** is the autocorrelation function of **R**.

Equation (9) can be written in matrix notation just as equation (4); however, the values of $A_{k-i,l-j}$ would have to be stored in a 4D matrix, the inversion of which is rather complicated. Tsokas and Papazachos (1992) tackled this point using a simple transform to reduce the order of the matrix. The same approach was followed in the present work.

The mathematical basis of the present work is very similar to that for total field measurements. The Geoscan Research FM256 magnetometer measures the vertical difference between two vertical component field values. This measurement can be represented by equation (1) provided that suitable modifications are made to the amplitude function $\mathbf{R}(x,y)$. First, the quantity c in equation (1) must be set to unity, to reflect the fact that the vertical field component is measured rather than the component along the main field direction. Second, the difference between the values of the function f at the two measurement heights must be substituted for the values of f in equation (1).

It is evident that the expression resulting from the substitutions described in the preceding paragraph still takes the form of equation (1). Thus, the convolutional model remains valid for this case and as a consequence so does the deconvolution equation (8). The matrices **R** and **D** now represent the differential shape and amplitude function, respectively. In fact, two vertical field shape functions are subtracted from each other in order to result in the differential shape function. As previously noted, the convolutional model does not change but only treats a different type of data in the same manner as the total field.

THE FORTRAN PROGRAM

The program that implements the convolution scheme calculates the inverse filter for the differential magnetic anomaly of an

oblique parallelepiped prism (Fig. 1) by constructing its shape function and inverting it. Next, it convolves the inverse filter with as many data sets as desired to produce the transformed versions, which are essentially magnetization maps.

The coordinate system used is of course the same as the one of the data grid and has its x and y axes horizontal, while the z axis is positive downwards. The fundamental format of the grid indices is the one of '-xOx and –yOy', i.e., the index x is changing more rapidly than index y. The input file index format is chosen throughout the process to avoid mixing rows with columns while all output files use the above-mentioned format (row scanning), with indices x and y ascending from 0 or 1 according to user's selection.

The prism is constructed by adjoining a number of thin plates, which can be selected by the user. All plates are considered to be of one common geometrical shape and magnetization. The geometrical features of the prism can be seen in Fig. 1. The prism's dip is measured by the angle φ. If this angle becomes 90^0 then the oblique parallelepiped prism becomes a vertical sided one with finite dimensions. Attention must be paid to the distances between the two sensors and the top of the prism. The vertical field shape functions are computed for two different heights and then subtracted from each other in order to produce the differential shape function.

The program can be divided in three parts:
In the first part the user inputs the sampling interval, the desired length of the inverse filter, the length of the autocorrelation function (for the computation only), the prism's geometrical features and the parameters of the ambient field. Special care should be taken when setting the number of thin plates, since large numbers both decrease the accuracy and increase the computation time. The lengths of the filter and autocorrelation function define essentially the dimensions of the involved matrices.

In the second part, the distances of the sensors to the upper surface of the prism are input. Then, the shape functions for the two heights are computed. Then, by simply subtracting the shape function of the upper sensor from the shape function of the lower sensor and multiplying it by the cosine of the inclination at the specific area, the final differential shape function is obtained. This is followed by the computation of its autocorrelation function. In FORTRAN code, they are then stored in the matrices **R'** and **A'** respectively. After rearranging their indices according to equations (8) and (9), they become the matrices RR and ALPHA.

Finally, in the third part, equation (10) is solved for $\overline{R}^{-1}$ (replaces **R'** in **RR** matrix in the program) using a simple Gauss-Jordan routine or a more sophisticated Levinson method routine. These routines can be found in Press *et al.* (1986). This is actually the operating part of the program where the filter (either computed or taken from another source) is applied to the data sets. This subroutine can be performed as many times as the number of data sets that need to be transformed. Construction of different filters for different cases is also possible. The program offers the possibility of storing the shape and autocorrelation functions in output files other than the filter and the magnetization map.

APPLICATION TO SYNTHETIC DATA

The performance of the proposed inversion scheme was tested on synthetic data. This was the initial test to verify how the program responds to anomalies caused by structures of which we possess detailed knowledge on their characteristics, both geometrical and magnetic. The targets in archaeological prospection comprise remnants of man-made structures and therefore they are usually well shaped in some geometrical form. Hence, most of them can be simulated by prisms without any particular difficulty and indeed, this is a good approximation to the shape of the buried targets. On the other hand, this justifies the employment of the vertical sided prism, having equal horizontal dimensions and depth extent as the basic model whose shape function will be computed and inverted to serve as a filter. In other words, the basic model whose effect will be inverted is nothing more than a cube, buried at shallow depths as is the usual situation in archaeological prospection.

The computation of the response of various simulations can be performed by the same program that is used for the construction of the inverse filters, since its first part is essentially a forward problem solver. Any desired simulation could be performed by combining several prisms like the one shown in Fig. 1. However, to be on the safe side, we preferred to use another algorithm to calculate the effect of the models. Thus, all the synthetic data (shown below) have been produced using the well-known algorithm of Talwani (1965) for the calculation of the response of 3D bodies.

Figure 2(a) shows the differential magnetic anomaly caused by a structure of cubic shape with sides of 1 m, buried at a 1 m depth (to its upper surface) and having a susceptibility contrast of 3.98×10^{-4} (SI). The used values of the magnetic inclination and declination are the ones standing for a Greek region i.e., 54^0 and 1.5^0 respectively. Wherever needed, these same values have been used throughout the whole process. The effect has been estimated supposing that the sensors of the gradiometer were placed at heights of 0.5 and 1 m above the ground surface. The plane view of the prism has been drawn as a continuous bold line in the same figure. The figure also shows the outcome after the application of an inverse filter to the magnetic anomaly. This particular inverse filter was constructed by the inversion of the shape function of an identical prism to the one whose anomaly is depicted in the left-hand part of the figure. On the other hand, the inverse filter was 5 x 5 square.

The magnetization magnitudes returned by the procedure were tested in order to confirm whether these values coincide with the ones theoretically expected. At the centre of the grid a differential field value of 7.7815 nT is transformed into a magnetization of 1.777×10^4 after the application of the inverse filter. Knowing that the susceptibility contrast is 3.98×10^{-4} (SI) and the

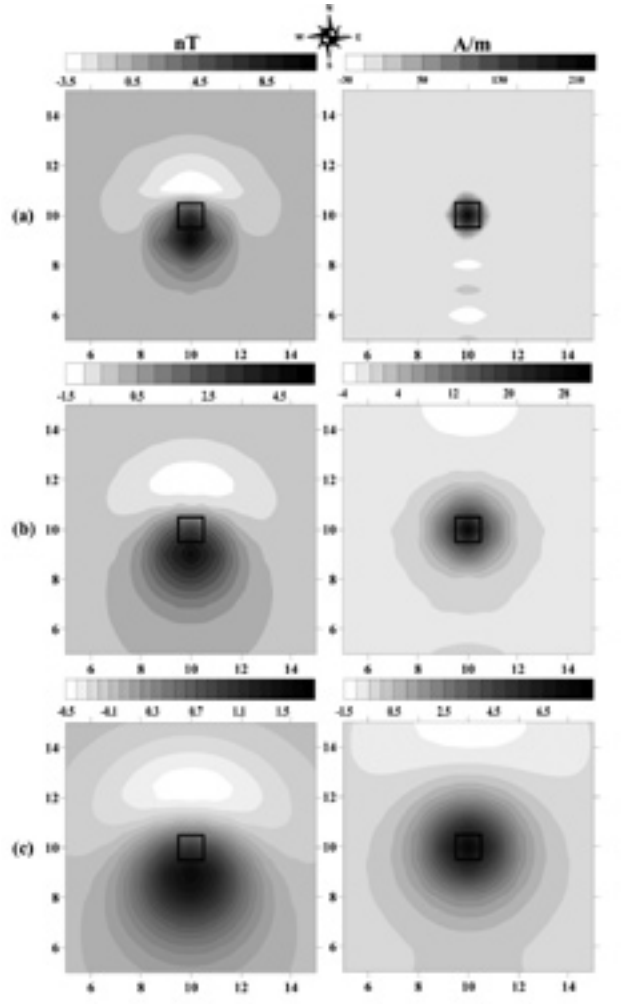

Figure 2
Case (a), left: magnetic anomaly map of a cubic prism (side = 1m, susceptibility contrast = 3.98 x 10^{-4} SI, magnetic declination and inclination values: D=1.5^0, I=54^0) buried at 1 m depth with its centre at point (10, 10) measured at sensor heights of 0.5 and 1 m. Case (a) right: corresponding magnetization map after the application of a 5 × 5 point filter designed for the disturbing body. In case (a), the filter has been constructed for the same depth as the model. In cases (b) and (c) the model has been translated to a depth of 2 and 3 m, respectively and the corresponding anomalies are shown on the left-hand side. Applying the same filter as in case (a), i.e., not a filter constructed for the correct burial depth, the results are shown on the right-hand side. It is evident that the outcomes are not indicative of the spatial extent of the bodies in the later cases. The filters have been constructed for the magnetic environment described above.

spacing between the sensors is 0.5 m, we were able to compute the theoretical value of the differential field at the specific point where a body of such magnetization is cited. The arithmetic result was 7.5996 nT, which is in very good agreement with the value 7.7815 nT previously noted. The small difference of

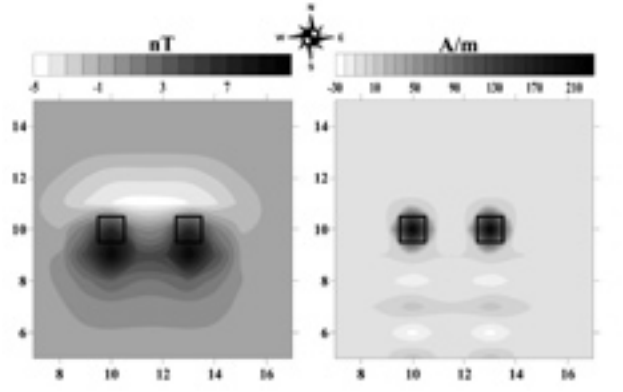

Figure 3
Left: magnetic anomaly map of two identical cubic prisms 2 m apart (side = 1m, burial depth 1m, susceptibility contrast = 3.98 × 10^{-4} SI, magnetic declination and inclination values: D=1.5^0, I=54^0) at sensor heights of 0.5 and 1 m. Right: corresponding map after the application of a 5 × 5 point filter.

0.1819 nT (2.3%) can easily be attributed to the mathematically different forward modelling solvers used as stated previously. Furthermore, full coincidence of values could have occurred only if an infinite series was involved as inversion theory implies and not truncated ones. Therefore, the resulting magnetizations confirm the theoretical background of the procedure.

The transformation of the differential anomaly yielded a form that resembles the plan view of the causative body. In other words, the lateral dimensions of the buried body are shown very well. Furthermore, the new form centred at the exact position of the projection of the centre of the buried body on the ground surface. Of course, the filter was constructed exactly for this specific case and so the result could only be successful.

An investigation of the influence of the wrong choice of the burial depth for the design of the filter is demonstrated in Figs 2(b) and 2(c). The filter remains unaltered, i.e., it is the inverted shape function of a cube with 1 m sides buried at a depth of 1 m. This particular filter is applied to the anomaly of an identical cubic structure but buried at a depth of 2 m. The anomaly and the result after the application of the filter are shown in Fig. 2(b). It is easily seen that the response does not have the desired properties described in the previous paragraph. The divergence from the desired properties is more pronounced as the burial depth of the cubic structure increases, as demonstrated in Fig. 2(c). In this last case, the body is buried at a depth of 3 m. Both these examples show that the pattern obtained broadens and reduces in magnitude as we move to greater depths when using a filter designed for shallower depth. The above investigations were performed and demonstrated for the total field case and demonstrated by Tsokas and Papazachos (1992). Tsokas (1993) also studied the same effect for the 1D total field case and presented a foundation for the explanation of the effect based on upward continuation. The same reasoning holds in the present

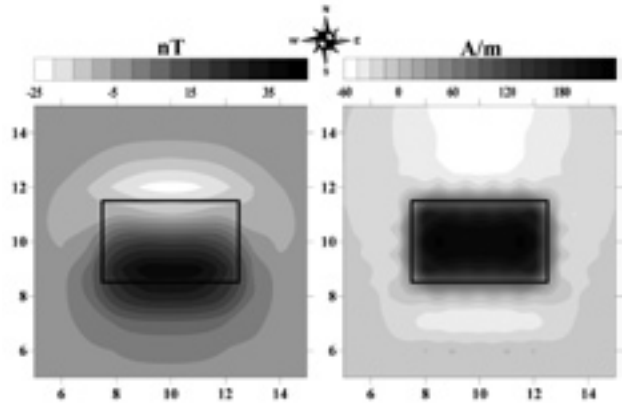

Figure 4
Left: magnetic anomaly map of a 5 × 3 m horizontal slab buried at 1 m depth at sensor heights of 0.5 and 1 m. Right: inversion result after the application of a 5 × 5 point filter.

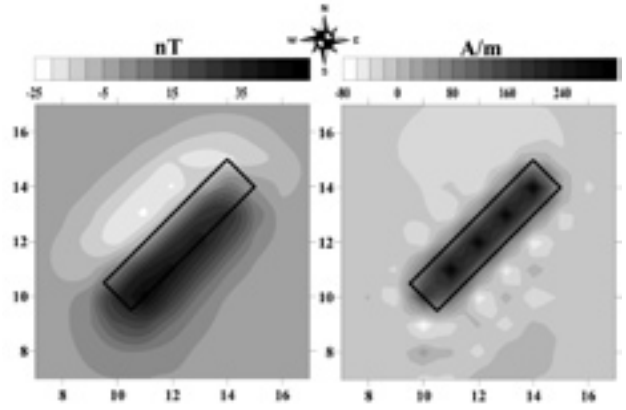

FIGURE 5
Left: magnetic anomaly map of a horizontal slab with its linear dimensions forming a 45^0 angle with the coordinate system, buried at 1 m depth and measured at sensor heights of 0.5 and 1 m. Right: resulting map after the application of a 5 × 5 point filter.

case of the differential field. The sources at an archaeological site are all likely to be at more or less the same depth and the depth of burial is also usually known beforehand.

Figure 3 shows the magnetic effect of two bodies identical to the one described above, buried 2 m apart and the result of the application of the inverse filter. It can be seen that the disturbing bodies have been revealed with their centres and dimensions delineated very well.

Figure 4 shows the magnetic gradient effect of a horizontal slab, 5 m long and 3 m wide and the result after its convolution with the same filter as the one used in the previous examples. The result is satisfactory since both the lateral dimensions of the slab and its actual position have been inferred. Note that the filter was constructed for a cube of 1 m dimensions. There was no inversion of the shape function of a 5 x 5 m^2 slab. The good performance of the filter for the anomaly of the slab is due to the

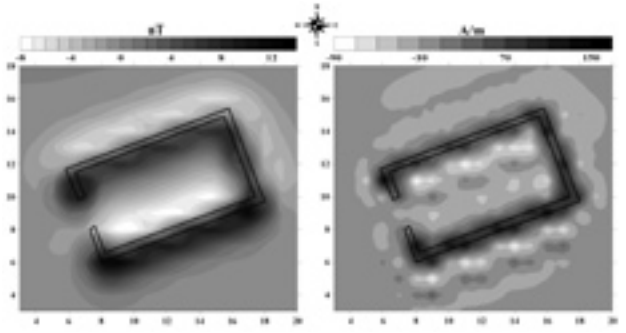

FIGURE 6
Left: magnetic anomaly map of the remains of an ancient building buried at 1 m depth at sensor heights of 0.5 and 1 m. Right: corresponding magnetization map after the application of a 5 × 5 point filter.

fact that the slab can be considered as composed of an ensemble of cubes.

Figure 5 shows the magnetic gradient effect of a slab with a NE orientation. This test aims to highlight the possible drawbacks that could be introduced if the structures are not along the directions defined by the coordinate system. The same filter as for the other tests has been applied to the data and its result can be seen in Fig. 5. Even though the filter has been constructed using the magnetic effect of a cube parallel to the coordinate system, the result has not been affected by the directional mismatch. The pattern resulting from inverse filtering has been translated into the correct position, i.e., it is now centred exactly over the source of the magnetic anomaly. Furthermore, the lateral extent of the slab is depicted quite well by the extent of the anomaly. This implies that the final image is not affected significantly if the initial prism used for the construction of the filter does not match the direction of the targets. Of course, there is always the capability of making the initial prism with the desired orientation.

The magnetic gradiometry effect of a model that simulates the buried ruins of the foundations of a building and the result after the application of the same inverse filter as before is shown in Fig. 6. The result is satisfactory in terms of the recovered dimensions of the buried structure and its actual location. The negative lobes have been eliminated, so that any depiction of the transformed field into image form would better resemble the actual features of the target.

The algorithm's efficiency in the presence of noise has been tested on the buried ruins model described above. The data were contaminated by adding Gaussian noise at three different levels, having maximum values of 0.5, 1 and 1.5 nT. Although the noise level may seem low with respect to the total field values, they are sufficiently high for the differential values, since they represent approximately 4, 8 and 12% of the maximum amplitude of the anomaly, respectively. In fact, a value of 0.5 nT implies a noise level of 1 nT per metre on our data, which shows that this amount of noise is actually significantly more than it seems. Thus, the percentage appearing on the top of each map on Fig. 7 refers to

the relation between the noise value and the maximum value met in our synthetic data. In other words, the noise level of 1 nT means that random values in the interval [-1, 1] nT were added to each data point.

The result of Fig. 7 shows that as the noise level increases, the image becomes more and more obscured. Furthermore, spurious effects appear in increasing numbers as noise increases. In general, the scheme is sensitive to noise in a modest way. The outline of the buried target is still visible at the noise level of approximately 8% as seen on the left-hand side of the lower part of Fig. 7. This fact implies that the proposed scheme is noise sensitive to high levels of noise. For reasonable levels of noise in the input, you obtain reasonable amounts of noise in the output. However, it is better applied cautiously in noisy data and avoided if the noise level is too high.

APPLICATION TO REAL DATA

Applying the algorithm to real data sets is the actual purpose of this work and will reveal the efficiency and potential of differential inverse filtering in rectifying possible targets of archaeological interest.

The example presented here comes from the archaeological site of Avgi, which lies in northwestern Greece (region of Macedonia, D=1.5^0 I=54^0). We have isolated two 20 m × 20 m grids of the significantly wider mesh established on the Earth's surface for the exploration of the site (Fig. 8). The survey was carried out by measuring along traverses spaced 0.5 m apart from each other stepwise at 0.5 m intervals. A FM256 gradiometer from Geoscan Research was used, having its lower sensor at 0.4 m height above ground level (Fluxgate magnetometer FM256; Instructions Manual 2003). Specifically, this particular instrument measures the first vertical difference of the vertical component of the field.

A well-shaped rectangular anomaly is observed in the measured grids that presumably reflects the presence of the ruins of foundations in this particular location. Note that the anomaly is positive, thus it is created by a feature more magnetic than the environment where it is buried, a fact that leads to the conclusion that the actual findings are most probably the trenches dug in the past to host the foundations of some structure. Although the random noise level is low, coherent noise is present due to ploughing tracks. The coherent noise has low amplitudes but due to the coherency, it manifests extremely well and it is superimposed on the signal. In fact, the presence of the ploughing tracks creates another type of noise also independent of the effect of the tracks themselves. The anomaly produced by the ploughing tracks is partly due to the soil piled next to the track and partly due to the trough, whose effect is compounded by the instrument height above the ground surface varying each time the operator crosses the shallow ditch.

Figure 8 shows the measured field with no further treatment. Several inverse filters were constructed for the case and applied to the raw data. After trials we concluded that the best performance was that of the filter computed by the inversion of the shape function of a cubic prism, having sides of 0.25 m and buried 0.5 m below the ground surface. The outcome of the application of the particular inverse filter is shown in Fig. 8.

We can see that the application of the filter has rectified the effect of the speculative structure. It is also useful to note that the algorithm has also amplified the effects of ploughing. This is a certain drawback of the technique, since its application will

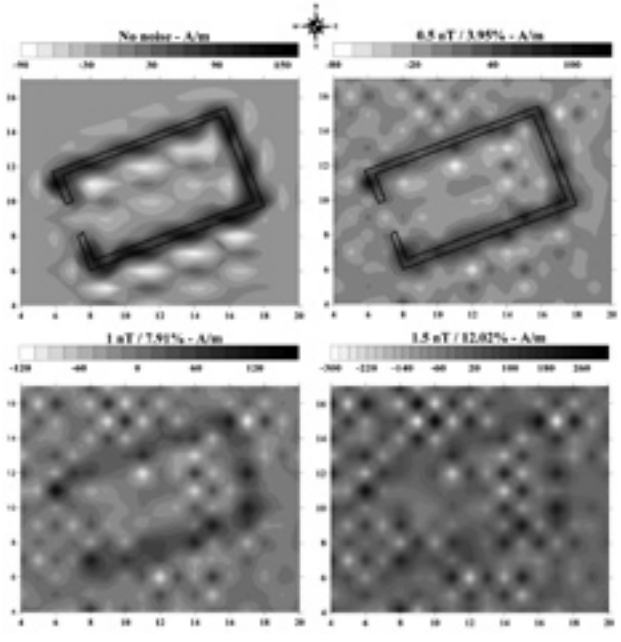

FIGURE 7

Magnetization maps after the application of the 5 × 5 filter for three different values of noise: 0.5, 1 and 1.5 nT.

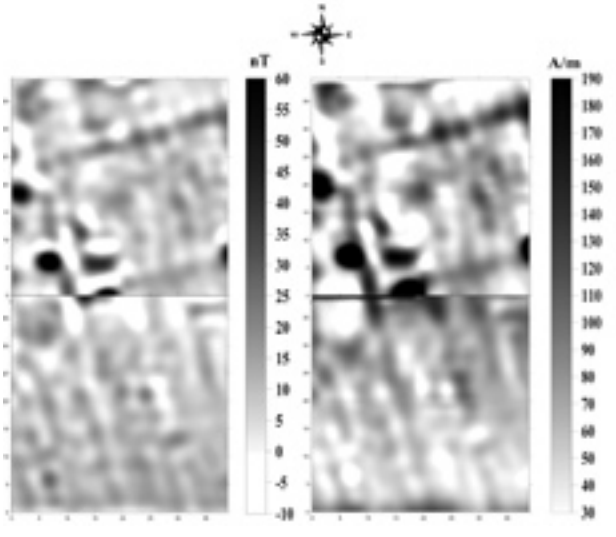

FIGURE 8

Left: distribution of the differential magnetic field in an area of 20 × 40 m at the site of Avgi (NW Greece). Right: the result of the convolution of the measured field with a cubic 9 × 9 filter.

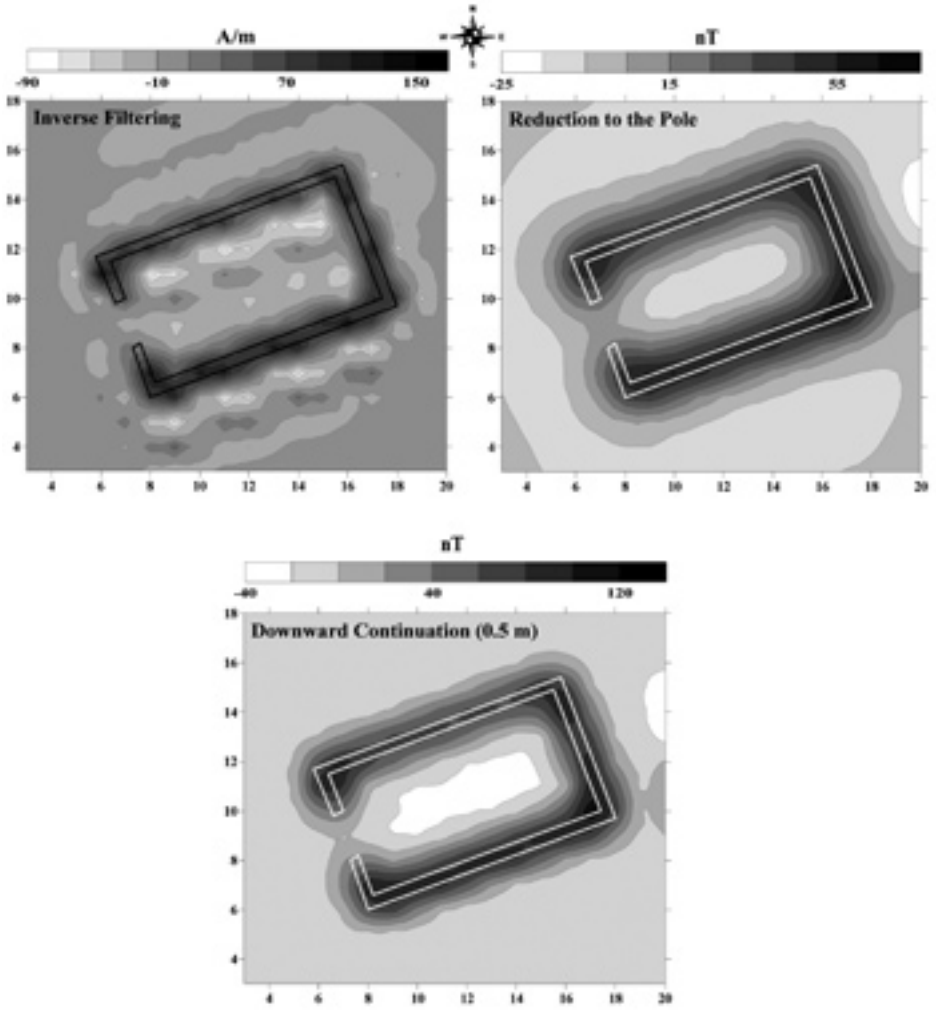

FIGURE 9
A comparison of the responses of inverse filtering and reduction to the north magnetic pole. Left: magnetization map after the application of a 5 × 5 point filter on the anomaly produced by the model whose plane view is depicted by the black line. The example is the same as in Fig. 6. The synthetic values of the differential field that were inverted data were computed for the sensors being at 0.5 and 1 m above the ground surface. Right: reduced to the pole, total magnetic field anomaly produced by the same model as in the example on the left-hand side. The synthetic total field was computed at 0.5 m above the surface. Lower part: the synthetic field that was previously reduced to the pole is continued further downward by 0.5 m. This process enriches the high frequency content and therefore results in an image more compatible to comparison with inverse filtering.

enhance any coherent noise present in our data. It would be beneficial to remove these spurious effects before the application of inverse filtering.

COMPARISON WITH REDUCTION TO THE POLE

Figure 9 demonstrates a comparison of the outcome of inverse filtering with reduction to the north magnetic pole. It shows the effects of both schemes as inferred from their application to the effect of the same model as the one used for the example in Fig. 6. The model simulates the buried ruins of foundation walls; the kind of buried structure that is most commonly met on archaeological sites.

It is easily seen that the final product, viewed as an image, is similar in both cases. However, the reduction to the pole results in a more blurry image in which the edges of the buried target are not clearly delineated. Generally, both approaches confront the requirement that the image should give the impression of the plan view of the buried antiquities. The demerit of the reduction to the pole is that it does not provide a direct estimate of the magnetization of the body, which is essentially what is mapped by inversion filtering. The reduction to the pole comprises a transformation of the field that raises one asymmetry while the proposed scheme is inversion based on certain considerations. The inverse filtering yields a magnetization mapping (or susceptibility mapping if we assume that magnetization is either purely of induced type or along a stable direction). In conclusion, we can say that these two schemes produce similar results from the point of view of an archaeologist but they comprise entirely different geophysical approaches.

The lower part of Fig. 9 shows the reduced to the pole field continued downwards by 0.5 m. This operation sharpens the high frequencies and its outcome therefore comprises an image that is more appropriate for the comparison with inverse filtering. It is obvious that no drastic changes exist with respect to the outcome of the reduction to the pole. Therefore, the reasoning referred in the previous paragraph also holds in this case.

DISCUSSION AND CONCLUSIONS

The performance of the application of inversion filters greatly depends on the depth and the dimensions of the initial model

whose shape function must be inverted. This model has to be designed such that its characteristics match those of the expected buried structures in the area under investigation. In fact, if elongated structures are expected, such as ruins of foundations, we need only one lateral dimension to be comparable, e.g., the width. This is because the simulation of the buried structure can be performed by combining a number of prisms identical to the initial model. If the buried structure is more like a slab, then the lateral dimensions do not have to match, provided that the initial prism has both dimensions much smaller than those of the slab. In this case, the test example of the slab showed that the result will be very good.

The choice of the correct depth is more crucial, i.e., the burial depth of the initial model should be close to the actual one of the buried structures. In quantitative terms, tests on synthetic data (Tsokas 1993; Tassis 2005) showed that the discrepancy must be at least less than half a measuring step (grid unit). In fact, small discrepancies of the order of 10–20% do not significantly affect the performance of the inverse filtering scheme. The assessment of the correct depth for the initial prism is not a particular problem in archaeological prospection. In most cases the burial depth of the expected concealed antiquities is known or it can be guessed in a good approximation.

The case of archaeological prospection being conducted in an area where nothing relevant to the expected antiquities is known is very rare. Even the crude dating of the surface pottery sherds is adequate in the majority of cases in order to yield a rough estimate of the expected burial depth.

The orientation of the initial prism has no detectable effect on the result of the proposed procedure. However, the prism can be made as we wish and of course we have the option to construct it such that its sides coincide with the directions defined by the axes of the system used or the direction of the structural directions of the subsurface targets. Moreover, there are cases where a single grid includes a number of linear structures of non-similar orientation. Then, the construction of a filter for a particular structure would of course slightly improve the result of the corresponding structure but at the same time, it would slightly degrade the signals of the other structures.

The scheme seems to be unaffected by low levels of random noise. However, it is definitely sensitive to medium to high noise levels. Thus, denoising of the data prior to the application of inverse filtering is strongly recommended. This approach can significantly reduce the appearance of spurious effects and enhance the performance of the subsequent application of inverse filtering.

The case of coherent noise seems to affect the transformation in a more severe manner. This is because inverse filtering will respond positively and the noise patterns will be enhanced instead of being suppressed. This effect increases proportionally to the increased complexity of the investigated structure. Of course, this would be the case with most of the processing schemes, except where particular filters are designed for the type of coherent noise present. A suitable treatment is to apply directional filtering in the wavenumber domain through Fourier transform or use wavelet schemes (Tsivouraki *et al.* 2005a; Tsivouraki and Tsokas 2005b, 2007).

Spikes and dummy value areas are not affected by the application of inversion filters. Thus, despiking is a minimum requirement and can be applied either before or after the application of the proposed scheme.

Furthermore, inversion filtering can be applied in order to reduce to the north magnetic pole data. Concerning total field data, the scheme of Tsokas and Papazachos (1992) can be directly used after suitable parameter setting. In case of differential data, either total field or vertical component, slight modifications of the present algorithm, are required.

In general, we can say that the convolution between differential magnetic data and differential inverse filters has been proven to perform satisfactorily. This success has also been met on the real data set of Avgi. Each application of the filters resulted in spatial distribution of the amplitude function, which by definition is the magnetization of the subsurface structures. In a different view, the proposed scheme comprises a technique for magnetization mapping. Since one of the assumptions was that the magnetization of the subsurface targets has to be along a stable direction or of induced type only, then the scheme also comprises a kind of susceptibility mapping.

A tailoring of the signal has been attempted, as it is the outcome of reduction to the pole, of the pseudogravity transformation or of ‘terracing’. This particular filtering is essentially equivalent to spiking deconvolution, which is a common processing step in reflection seismics. The new, transformed versions of the original signals are monopolar, having maximum values exactly above the centres of the buried bodies and their lateral dimensions matching more or less those of the bodies. Of course there are still some drawbacks, concerning mainly the destructive influence of noise. However, in many cases, where the scheme would perform satisfactorily, the outcome is more suitable for subsequent image presentation of the data. It should be borne in mind that the most desired outcome of any archaeological prospection is to finally provide an image that resembles the drawing of the antiquities that would had been executed after the excavation. In this context, inversion filters offer correct positioning and rectification, i.e., an image that is closer to the drawing than the image of the original data.

ACKNOWLEDGEMENTS

This research was funded by the Ministry of Education under the O.P. Education II programme “Pythagoras II – Support to Research Teams in the Universities”.

REFERENCES

Aspinall A. and Lynam J.T. 1973. An induced polarization instrument for the detection of near surface features. *Prospezioni Archaeologiche* **5**, 67–75.

Baranov V. 1957. A new method for interpretation of aeromagnetic maps: pseudo-gravimetric anomalies. *Geophysics* **22**, 359–383.

Baranov V. and Naudy H. 1964. Numerical calculation of the formula of reduction to the magnetic pole. *Geophysics* **29**, 67–79.

Blakeley R.J. 1995. *Potential Theory in Gravity & Magnetic Applications*. *Cambridge University Press.*

Cordell L. and McCaffery A.E. 1989. A terracing operator for physical property mapping with potential field data. Geophysics **54***, 621–634.*

Daubechies I. 1990. The wavelet transform, time frequency localization and signal analysis. *IEEE Transactions on Information Theory* **36**, 961–1005.

Fedi M. and Quarta T. 1998. Wavelet analysis for the regional - residual separation of potential field anomalies. *Geophysical Prospecting* **46**, 507–525.

Fleming B.J.W., Yu D., Harrison R.G. and Jubb D. 2000. Analysis of effect of detrending time-scale structure of financial data using discrete wavelet transform. *International Journal of Theoretical and Applied Finance* **3**, 375–380.

Fluxgate gradiometer FM256. 2003. *Instruction Manual Version 1.2.* Geoscan Research.

Grant F.S. and West G.F. 1965. *Interpretation Theory in Applied Geophysics.* McGraw-Hill, New York.

Hansen R.O. and Simmonds M. 1993. Multiple source Werner deconvolution. *Geophysics* **58**, 1972–1800.

Hartman R.R., Teksey D.J. and Friedberg J.L. 1971. A system for rapid aeromagnetic interpretation. *Geophysics* **36**, 891–918.

Kanasewich E.R. 1981. *Time Sequence Analysis in Geophysics*. University of Alberta Press, Edmonton.

Karousova O. and Karous M. 1989. Deconvolution of ΔT profile curves. International Symposium on Computer Applications and Quantitative Methods in Archaeology, University of York and York Archaeological Authorities.

Logacev A.A. and Zacharov V.P. 1973. *Magnetic Prospecting*. Moscow (in Russian).

Mallat S. 1999. *A Wavelet Tour of Signal Processing*. Academic Press.

McGrath P.H. and Hood P.J. 1973. An automatic least-squares multimodel method for magnetic interpretation. *Geophysics* **38**, 349–358.

Papazachos C.B. and Tsokas G.N. 1993. A FORTRAN program for the computation of 2-dimensional inverse filters in magnetic prospecting. *Computers & Geosciences* **19**, 705–715.

Press W.H., Teukolsky S.A., Vetterling W.T. and Flannery B.P. 1986. *Numerical Recipes – The Art of Scientific Computing, 1st Ed.* Cambridge University Press.

Reid A.B., Allsop J.M., Granser H., Millet A.J. and Somerton I.W. 1990. Magnetic interpretation in three dimensions using Euler deconvolution. *Geophysics* **55**, 80–91.

Roest W.R., Verhoef J. and Pilkington M. 1992. Magnetic interpretation using the 3D analytic signal. *Geophysics* **57**, 116–125.

Scollar I., Weidner B. and Segeth K. 1986. Display of archaeological magnetic data. *Geophysics* **51**, 623–633.

Talwani M. 1965. Computation with the help of a digital computer of magnetic anomalies caused by bodies of arbitrary shape. *Geophysics* **30**, 797–817.

Tassis G.A. 2005. *MSc. Thesis: Inversion of differential magnetic data in the exploration of archaeological sites*. PhD thesis. Applied Geophysical Laboratory, Aristotle University of Thessaloniki.

Tsivouraki-Papafotiou B., Tsokas G.N. and Tsourlos P.I. 2005a. Wavelet denoising of magnetic prospecting data. *Journal of the Balkan Geophysical Society* **8**, 28–36.

Tsivouraki-Papafotiou B. and Tsokas G.N. 2005b. Wavelet transform in denoising magnetic archaeological prospection data. 6th Conference of Archaeological Prospection, Rome, September 14–17.

Tsivouraki-Papafotiou B. and Tsokas G.N. 2007. Wavelet transform in denoising magnetic archaeological prospection data. *Archaeological Prospection* **14**, 130–141.

Tsokas G.N. 1993. An investigation of the effectiveness of inverse filtering in the geophysical search of archaeological sites. *Theory and Practice of Applied Geophysics* **7**, 73–88.

Tsokas G.N. and Hansen R.O. 1995. A comparison of inverse filtering and multiple source Werner deconcolution for model archaeological problems. *Archaeometry* **37**, 185–193.

Tsokas G.N. and Hansen R.O. 2000. On the use of complex attributes and the inferred source parameter estimates in the exploration of archaeological sites. *Archaeological Prospection* **7**, 17–30.

Tsokas G.N. and Papazachos C.B. 1990. The applicability of two-dimensional inversion filters in magnetic prospecting for buried antiquities. In: Theory and Practice of Geophysical Data Inversion (eds A. Vogel, A.K.M. Sarwar, R. Gorenfio and O.I. Kounchev), pp. 121–144. Vieweg Verlag, Wiesbaden.

Tsokas G.N. and Papazachos C.B. 1992. Two-dimensional inversion filters in magnetic prospecting: application to the exploration of buried antiquities. *Geophysics* **57**, 1004–1013.

Tsokas G.N., Papazachos C.B., Loucoyiannakis M.Z. and Karousova O. 1991. Inversion filters for the transformation of geophysical data from archaeological sites based on the vertical sided finite prism model. Archaeometry **33***, 215–230.*